Stability of Equal-leg Angle Steel Columns with Single-clad End Connection Joints

Liang Zhu [1]*, Xing Huang [3], Zhengliang Li [1, 2], and Hongjun Liu [1, 2]

[1] College of Civil Engineering, Chongqing University, Chongqing, China; Email: lizhengl@hotmail.com (Z.L.L.), LHJ20040308@126.com (H.J.L.)

[2] Key Laboratory of New Technology for Construction of Cities in Mountain Area of Ministry of Education, Chongqing University, Chongqing, China

[3] Southwest Electric Power Design Institute, Chengdu, China; Email: 764016880@qq.com (X.H.)

*Corresponding author: huliang971@163.com (L.Z.)

***Abstract*—Angle steel columns with connection joints are prevalent in tower structures, and their stability bearing capacity directly determines the safety of the towers. The bearing capacity and structural performances of Q355 equal-leg angle steel columns with Single-Clad End Connection joints (SCEC) were analyzed based on axially loaded experiments and numerical simulations. Experimental setup and procedures have been described in detail. Typical test results of 30 columns were reported and analyzed, including failure modes, load-axial deformation curves, load-lateral displacement curves, and load-strain curves. Combined with the results of the test and the finite element analysis, it was found that the local buckling mode dominates in the angle columns with SCEC when $\lambda < 120$ (herein λ is the slenderness ratio), while the flexural buckling mode dominates when $\lambda \geq 120$. The overlap area ratio is recommended to be not less than 1.1. The length of connection joints has a positive correlation to the bearing capacity of the short columns with SCEC. The bearing capacity of stockier columns with SCEC is lower than that of the single angle columns to varying degrees, the slenderer ones is slightly higher than that of the single angle columns. With the slenderness ratio continuing to increase, the bearing capacity of angle columns with SCEC is getting closer to that of single angle columns. The predictions of relevant design codes are excessively conservative in the moderate-to-high λ range, while the result was the opposite for the specimens with a smaller λ.**

***Keywords*—Tower structures, equal-leg angle steel columns, connection joints, axially loaded experiments, bearing capacity**

I. Introduction

The economic development and citizens' daily life are inseparable from the stable supply of electric powers, angle steel towers are the common supporting structures in the process of power transmission, and the study of its structural performance is always of great significance.

The connection joints of angle columns are inevitable in angle steel towers due to the limitations of manufacturing, transportation and hoisting efficiency. The angle columns and cross-bracings in transmission towers are usually composed of several equal-leg angle steel connected by connection joints [1]. The full-scale tower test [2] shows that the failure of the transmission towers is related to the connection joints of angle columns, and local buckling of the angle columns with connection joints may occur before the design load is reached. Owing to the particular characteristic of the angle columns with end connection joints in transmission towers, there is an urgent need for the exploration of its compression resistance.

Angle steel has been widely employed in transmission towers because of its simple production process, easy connection and lower cost of materials. Several scholars conducted in-depth studies on the stability bearing capacity and failure modes of angle steel columns under compression. The failure modes of equal-leg angle steel columns always exhibit local, flexural, and flexural–torsional buckling modes or their combination [3–6]. Chen *et al.* [7–8] studied the test data of single angle steel columns and provided the recommended calculation formula for the bearing capacity of angle steel in combination with the American design codes. Li *et al.* [9–11] conducted a series of tests on Q460 high-strength angle columns. It was shown that the bearing capacity of angle columns under the axially compressed test was much greater than the predictions of relevant design codes when the slenderness ratio exceeded 60. Huang *et al.* [12] experimentally investigated the structural behaviors and resistances of single equal-leg angle columns under three typical end constraints and evaluated the applicability of several design codes. Jiang *et al.* [13] studied the bearing capacity of angle columns with connection joints through finite element analysis. It was found that the bearing capacity of angle columns with end connection joints was 35% lower than that of the single angle columns without connection joints, and the smaller the slenderness ratio, the larger the bearing capacity decreases.

To the best of the authors knowledge, many compression tests for the single angle columns in published literature have not sufficiently consider the

Manuscript received February 8, 2023; revised April 17, 2023; accepted July 30, 2023.

spatial boundary conditions of the angle columns in transmission towers. Few test studies on angle columns with end connection joints have been conducted. Regarding the design of angle steel towers, the provisions for predicting the bearing capacity of single angle columns in international codes also does not appropriately consider the influence of connection joints.

In this study, Experiments and numerical simulations were conducted to investigate the structural behaviors and compression resistances of angle columns with single-clad end connection joints. The compression test includes 30 columns, and simultaneously refined Finite Element Models (FEMs) were established and validated against the test results. Consequently, an extensive parametric analysis was conducted by considering a wide range of influential parameters, including overlap area ratios, length of connection joints, slenderness ratios. Finally, some suggestions for the design of angle columns with single-clad end connection joints was proposed by the test observation and numerical simulations.

II. Experimental Study

A. Test Specimens

Angle columns with connection joints are prevalent in tower structures, as shown in Fig. 1, the position of the connection joints of angle columns is also almost at the end of the internode in transmission towers. According to DL/T5154–2012 [14], the dimensions of equal-leg angles should not be less than 40 × 40 × 3. The double-clad connection joints is recommended to jointing angle columns. The leg width of the connection angle steel should be wider than that of angle columns while the single-clad connection joints is used. When the dimensions of angle steels columns are small, it is more convenient to use the single-clad end connection joints (SCEC) due to its simplicity and economy. Large-dimension angle columns are more commonly connected by the double-clad end connection joints (DCEC) owing to the larger bear capacity. Therefore, a type of Q355 high-strength steel equal-leg-angle sections (90 × 90 × 7) selected from the design database of the Chinese State Grid were included in the test specimens. The test specimens included single angle columns and angle columns with SCEC (see Fig. 2).

The overlap area ratio (A) is defined as the ratio of the cross-sectional area of the connection angle steel to that of the angle columns. S is the slenderness ratio. b is the distance of bolts, which determines the length of the SCEC. N for the number of single-leg bolts (a quarter of the total number of bolts at the connection joints). Table I lists the specimen groups (each group contains three same specimens) with their section size, slenderness ratio and the overlap area ratio. Three column specimens with the same nominal section size, length and overlap area ratio were set in each group and each specimen was designated a label containing its main testing parameters. Take S80D400A1.1 as an example, 80 is the slenderness ratio(S); 400 is the length of the connection joints (D) and the unit is millimeters; 1.1 is the overlap area ratio (A). S120 indicate the single angle columns. The labels of these column specimens are listed in Table I.

B. Experimental Setup and Procedures

To simulate appropriately the boundary conditions of angle columns in transmission tower, four angle steels (63 × 63 × 5, Q355, of length 1000 mm) perpendicular to the angle column were selected in this study as the support angle steel. One end of the support angle steel is connected to the angle column using high-strength bolts of diameter 16 mm, and the other to the static frame with a strip-shaped hole using high-strength bolts of diameter 20 mm. It should be noted that the strip-shaped hole was set to release the movement along the loading direction.

High-strength bolts of diameter 20 mm are used for end connection joints of the angle columns. Both ends of the specimen were concentrically loaded with spherical hinges. Extensions of 2/3 length of the internode segment are made at the ends, in order to eliminate the effect of stress concentration at end constraints and to better simulate the realistic spatial boundary conditions in transmission towers. The slenderness ratio of specimens which is defined as the length of the internode segment divided by the radius of gyration about the minor principal axis. The relative experimental studies in published literature have rarely focused on authentic end constraints of angle columns in practical engineering. The difference in this study is that the end constraint of internode segment can be regarded as elastic constraints since the specimens are connected with support angle steel by bolts. The experimental setup is shown in Fig. 3.

In the loading process, the specimen was subjected to a monotonically increasing load in steps after a pre-load process. A pressure transducer with an appropriate range was fixed between the specimen and the jack for measurement of the bearing capacity. Several locations, such as the mid span and 3/4 span of internode segment, etc., were selected as measuring points for measuring the deformation and strain distribution.

Before the loading tests, tensile tests were conducted to measure the material properties, including the yield stress, ultimate stress and elastic modulus. The actual cross-sectional area of each specimen was also measured using the weighing method. The tensile test and the four typical stress-strain curves are shown in Fig. 4. Material parameters of specimens are taken from the average values of test results.

TABLE I. Test Specimens and Their Properties

Specimens	S	A	b (mm)	N	Type of specimens
S80 D400A1.1	80	1.1	90	2	Angle columns with SCEC
S80 D454A1.1	80	1.1	108	2	
S80 D535A1.1	80	1.1	135	2	
S120 D400A1.1	120	1.1	90	2	
S120 D454A1.1	120	1.1	90	2	
S120 D535A1.1	120	1.1	135	2	
S160 D400A1.1	160	1.1	90	2	
S160 D454A1.1	160	1.1	108	2	
S160 D535A1.1	160	1.1	135	2	
S120	120	-	-	-	Single angle columns

C. Failure Modes

The specimens of slenderness ratio 80 did not exhibit evident flexural deformation in the early loading phase. When the test load reached 125 kN, loud sounds were generated during the loading process due to the bolt slippage. When the load reached 215 kN, the specimens suddenly failed due to local buckling near the mid-span section and the load decreased abruptly. Irrecoverable residual plastic deformation was observed after unloading. The typical observations are shown in Fig. 5(a).

For the specimens of slenderness ratio 160, bolts slippage began to occur at the connection joints when the test load reached 100 kN. With an increase of load, the flexural deformation about the minor principal axis slowly increased along with the slightly inclining spherical hinge bearing. Upon approaching the critical state, considerable bending deformation occurred in the mid-span section without any observed torsional deformation, henceforth the load began to decrease slowly. Finally, the specimen performed with a flexural buckling mode, as shown in Fig. 5(b). Substantial elastic deformation was recovered after unloading.

For the specimens of slenderness ratio 120, the failure modes of the specimens were mainly flexural buckling with insignificant torsion. The local buckling occurred in mid-span section was observed only once (see Fig. 5(c)), it may be caused by excessive compression during the test. There was almost no difference in bearing capacity between the two failure modes. On the other hand, all the single angle columns of slenderness ratio 120 performed flexural buckling, the Fig. 5(d) shows the failure modes of the single angle columns.

Typical specimens were selected for analyzing the relevant strain and displacement curves. As shown in Fig. 6(a), the axial deformation of specimens S160D400A1.1 increased faster than that of specimens S80D400A1.1 in the early loading phase. Displacement curves are not smooth enough due to the bolt slippage at the connection joints and the vibration of the specimens during the loading process. Fortunately, the bear capacity and post-buckling results were not influenced. Fig. 6(b) shows the lateral displacements of specimens S80D400A1.1 measured at the two legs of the angle column in the mid-span section. Meanwhile, the strains measured at points 1 and 4, as shown in Fig. 6(c), exhibited the absolutely opposite trend after approaching the critical state, which means, the angle columns of specimens of slenderness ratio 80 failed in a local buckling mode. During the unloading phase, the lateral displacement and strain decreased slightly but cannot recover to the initial stress-free state. On the other hand, the specimens of slenderness ratio 160 failed in a flexural buckling mode.

D. Stability Bearing Capacity

The failure modes and stability bearing capacity obtained from the test were sorted, and the average value of them and typical failure modes are taken for analysis. As shown in Table II, ZL denotes the local buckling in the mid-span section, FB denotes the flexural buckling. Note that the specimens S120 D454A1.1 only failed in a local buckling once.

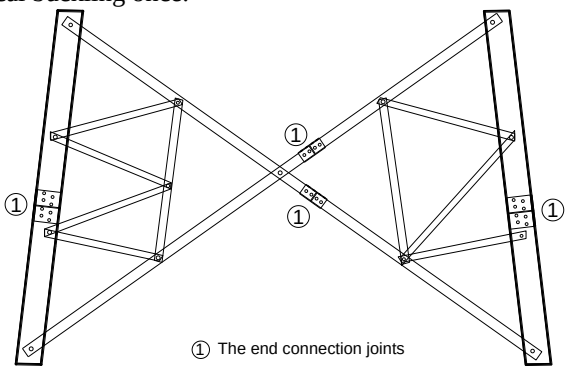

Figure 1. The internode in the transmission towers.

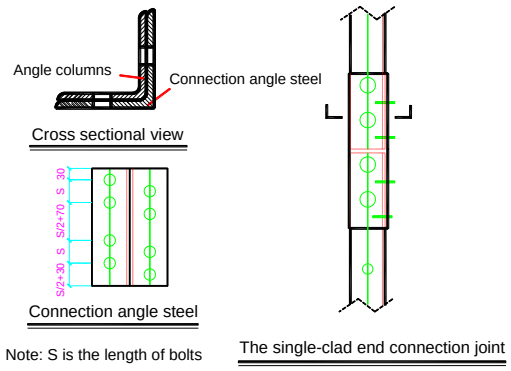

Figure 2. The single-clad end connection joints (SCEC).

Figure 3. The experimental setup.

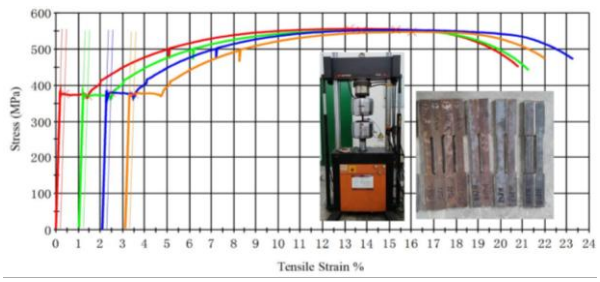

Figure 4. Tensile test and typical stress-strain curves.

(a) The specimens with a slenderness ratio of 80

(b) The specimens with a slenderness ratio of 160

(c) The specimens with a slenderness ratio of 120

(d) The single angle columns (S120)

Figure 5. Typical failure modes of specimens

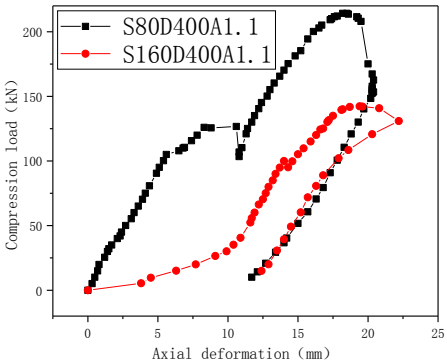

(a) The load-axial deformation curve

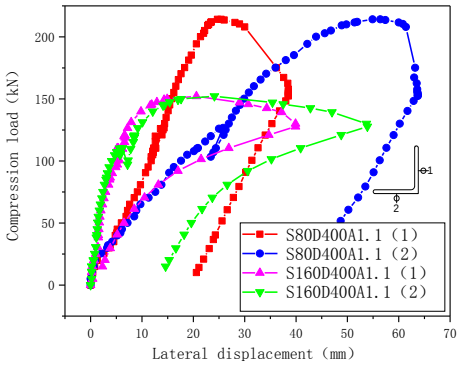

(b) The load-lateral displacement curve of the mid-span section

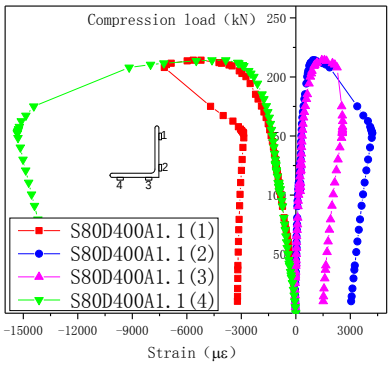

(c) The load-strain curve of mid-span section (S80D400A1.1)

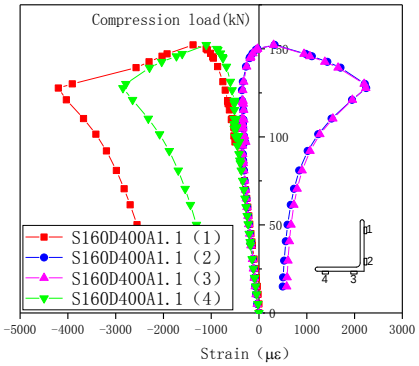

(d) The load-strain curve of mid-span section (S160D400A1.1)

Figure 6. Load-displacement and load-strain curves of specimens

TABLE II. COMPARISON OF BEARING CAPACITY OF THE TEST AND THE PREDICTION OF DESIGN CODES

Specimens	Failure modes	P_E (kN)	$(P_E - P_{code})/P_E$
S80 D400A1.1	ZL	213.9	-17.95
S80 D454A1.1	ZL	214.8	-17.45
S80 D535A1.1	ZL	236.1	-6.86
S120 D400A1.1	FB	200.9	30.95
S120 D454A1.1	FB, ZL	211.2	34.32
S120 D535A1.1	FB	226.9	38.86
S160 D400A1.1	FB	154.4	45.80
S160 D454A1.1	FB	153.5	45.48
S160 D535A1.1	FB	143.4	41.64
S120	FB	192.7	28.01

To better illustrate, the relative error rate defined as $(P_E - P_{code})/P_E$, where P_E is the average value of bearing capacity of specimens, P_{code} is the predictions based on DL/T5154-2012.

It was found that the bearing capacity of the stockier columns with SCEC was less than the predictions of codes and that of slenderer columns with SCEC was much greater than the predictions of codes. The bearing capacity of angle columns with SCEC was greater than that of single angle columns (S120). The length of connection joints has certain influence on the stability bearing capacity of the angle columns with SCEC. The length of the connection joints is positively related to the stability bearing capacity of the specimens with slenderness ratio of 80 and 120. This law was not detected at the slenderness ratio of 160 due to the existence of experimental errors during the test. It is necessary to reveal the effect laws of length of the connection joints through finite element analysis.

III. FINITE ELEMENT ANALYSIS

A. Establishment and Validation of Models

In parallel with the test, a careful numerical simulation was followed using the finite element software ANSYS. Solid element Solid185 was employed to simulate the angle columns and connection joints. The Bilinear Kinematic Hardening Model (BKIN) with tangential modulus of E_t=0.02E was adopted as constitutive relation of steel. The average values of elastic modulus E, yield strength f_y, Poisson ratio v, and ultimate strength f_u from the tensile test of material properties were used for the finite element model. The nodes of bolts were coupled with screw hole with the in-plane rotation freed, in order to achieve more efficient analysis.

The typical failure modes of FEM are the same as those obtained from the tests, as shown in Fig. 7. Table III lists the comparison between the bearing capacities obtained from the FEM (Pa) and experiments (P_E). A mean value for the ratio Pa/P_E of 1.066 indicates that the bearing capacity of the tested specimens could be accurately predicted by the FEM. Therefore, the capacity of such finite element models to perform parametric studies covering a wide range of data can be confirmed.

B. Parametric Studies

For the specimens (90 × 90 × 7) with a slenderness ratio of 80, different overlap area ratios were set for parametric analysis to study the influence of it on the failure modes and their bearing capacity. Fig. 8 shows the relationship between the bearing capacity and overlap area ratio. The bearing capacity of specimens gradually increases and then flattens with the increase of the overlap area ratio. The specimens with an overlap area ratio of 0.9 performed strength failure of connection joints (see Fig. 9), while the specimens with an overlap area ratio of 1.0 and above exhibited local buckling in mid-span section. However, the increasing trend of the bearing capacity of the specimens is no longer significant when the overlap area ratio exceeds 1.1. It is suggested that the overlap area ratio of the connection joints should not be less than 1.1, and the subsequent parametric analysis will be based on the specimens with overlap area ratio of 1.1.

The results of bearing capacity obtained by Finite element simulation are compared with that of two domestic design codes [14–15]. As shown in Fig. 10, The abscissa is the regularized slenderness ratio λ_n, the ordinate is the stability coefficient φ.

$$\lambda_n = \lambda / \pi \sqrt{f_y / E} \ . \tag{1}$$

$$\varphi = N / A f_y \ . \tag{2}$$

where λ is the slenderness ratio of specimens, which is determined by S in label of specimens. f_y, E is the yield stress and elastic modulus obtained by tensile test respectively. N in (2) is the bearing capacity of finite element models. A is the actual cross-sectional area of each specimen measured by the weighing method, A in (2) is not the overlap area ratio, so it should be distinguished.

The angle columns with SCEC with the slenderness ratio less than 120 exhibited the local buckling, while the other specimens performed flexural buckling. The bearing capacity of the angle columns with SCEC increases gradually and then flattens with the decrease of the slenderness ratio. The longer the length of connection joint (D), the greater the bearing capacity of short columns with SCEC. However, the influence of length of SECE on bearing capacity is no longer obvious when the slenderness ratio is large. Therefore, it is recommended to use longer connection joints on short columns.

TABLE III. VALIDATION OF THE FINITE ELEMENT RESULTS

Specimens	Failure modes	P_E (kN)	P_a (kN)	P_a/P_E
S80 D400A1.1	ZL	213.9	232.5	1.09
S80 D454A1.1	ZL	214.8	243.2	1.13
S80 D535A1.1	ZL	236.1	254.1	1.08
S120 D400A1.1	FB	200.9	213.2	1.06
S120 D454A1.1	FB	211.2	220.1	1.04
S120 D535A1.1	FB	226.9	230.9	1.02
S160 D400A1.1	FB	154.4	155.5	1.00
S160 D454A1.1	FB	153.5	158.3	1.03
S160 D535A1.1	FB	143.4	160.1	1.11
S120	FB	192.7	212.0	1.10

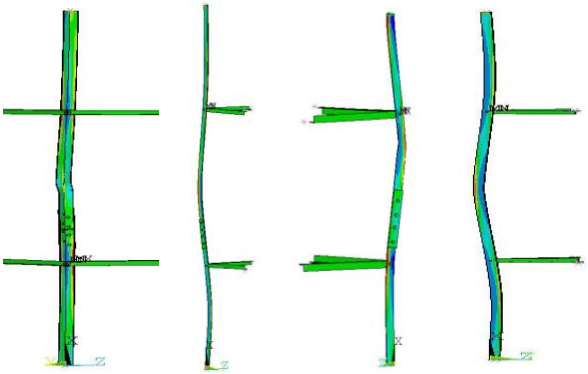

Figure 7.The typical failure modes of finite element models.

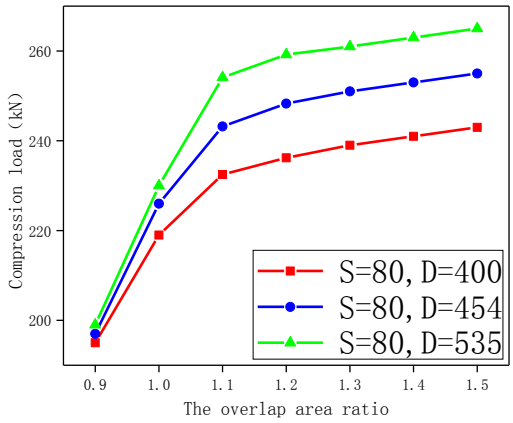

Figure 8. The bearing capacity-overlap area ratio relations.

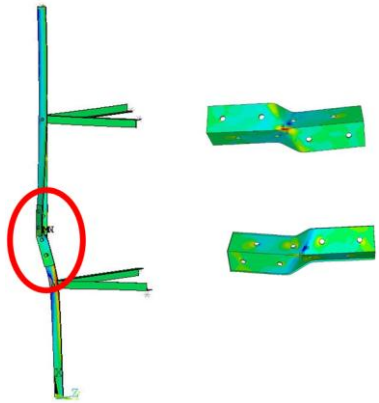

Figure 9. The strength failure of connection joints.

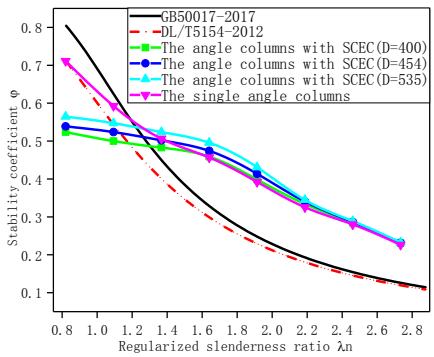

Figure 10. Effect of slenderness ratio on the stability coefficient φ.

As shown in Fig. 10, the stability bearing capacity of angle columns with SCEC ($\lambda_n \leq 1.2$) is lower than that of the single angle columns to varying degrees. However, the bearing capacity of angle columns with SCEC ($\lambda_n \geq 1.6$) is slightly higher than that of the single angle columns. With the slenderness ratio continues to increase beyond $\lambda_n \geq 2.0$, the bearing capacity of angle columns with SCEC was almost the same as that of single angle columns.

For the angle columns with SCEC, the bearing capacity of the specimens with a small slenderness ratio is lower than the value predicted by codes to varying degrees, which is mainly caused by the local buckling. While the bearing capacity values of those specimens with a larger slenderness ratio are almost all above the two code- based prediction curves, indicating that the two design codes provide conservative predictions. The results are similar with the experimental conclusion of the Ref. [3] and Ref. [10].

IV. Conclusions

The stability bearing capacity and failure modes of Q355 equal-leg angle steel columns with Single-Clad End Connection joints (SCEC) were analyzed based on axially loaded experiments and effective finite element models. Based on all the research results, the following conclusions were drawn:

(1) The single angle columns performed flexural buckling in this test. Combined with the test and the finite element results, the local buckling mode dominates in the angle columns with SCEC when $\lambda < 120$, while the flexural buckling mode dominates when $\lambda \geq 120$. The predictions of relevant design codes are excessively conservative in the moderate-to-high λ range, while the result was the opposite for the specimens with a smaller λ.

(2) The parametric analysis indicates that the bearing capacity of specimens gradually increases and then flattens with the increase of the overlap area ratio. The overlap area ratio is too small to ensure the stiffness of the connection joints, it is recommended to be not less than 1.1.

(3) The length of connection joints has a positive correlation to the bearing capacity of the short columns with SCEC. The bearing capacity of stockier columns with SCEC is lower than that of the single angle columns to varying degrees, the slenderer ones is slightly higher than that of the single angle columns. With the slenderness ratio continuing to increase, the bearing capacity of angle columns with SCEC is getting closer to that of single angle columns.

Conflict of Interest

Disclosure statement: on behalf of all authors, the corresponding author states that there is no conflict of interest.

AUTHOR CONTRIBUTIONS

Liang Zhu conducted data curation, manuscript writing and software application; Xing Huang provided resources and funding acquisition; Zhengliang Li and Hongjun Liu conducted article editing, proofreading and data validation; all authors had approved the final version.

ACKNOWLEDGMENTS

This research project was fully funded by the Fundamental Research Funds for Hubei Transmission Line Engineering Technology Research Center (China Three Gorges University) (No. 2019KXL01) and the Southwest Electric Power Design Institute of China Power Engineering Consulting Group (GSKJ2-T08-2019). The authors would like to express their gratitude for all generous financial sponsorship.

REFERENCES

[1] W. Q. Jiang, Z. Q. Wang, G. McClure, G. L. Wang, and J. D. Geng, "Accurate modeling of joint effects in lattice transmission towers," *Eng. Struct.*, vol. 33, no. 5, pp. 1817-1827, 2011. doi:10.1016/j. engstruct.2011.02. 022.

[2] L. Tian, H. Pan, R. Ma, L. Zhang, and Z. Liu, "Full-scale test and numerical failure analysis of a latticed steel tubular transmission tower," *Eng. Struct.*, vol. 208, 2020, 109919. doi: 10.1016/j.engstruct.2019. 109919.

[3] A. Filipovic, J. Dobric, N. Baddoo, and P. Moze, "Experimental response of hot-rolled stainless steel angle columns," *Thin-Walled Struct.*, vol. 163, 2021, 107659. doi:10.1016/j.tws.2021. 107659.

[4] A. Filipovic, J. Dobric, D. Budevac, N. Fric, and N. Baddoo, "Experimental study of laser-welded stainless steel angle columns," *Thin-Walled Struct.*, vol. 164, 2021, 107777. doi:10.1016/ j.tws.2021.107777.

[5] B. Young and E. Ellobody, "Design of cold-formed steel unequal angle compression members," *Thin-Walled Struct.*, vol. 45, no. 3, pp. 330–338, 2007. doi:10.1016/j.tws.2007.02.015.

[6] L. Zhang, Y. Liang, and O. Zhao, "Laboratory testing and numerical modelling of pin-ended hot-rolled stainless steel Angle section columns failing by flexural-torsional buckling," *Thin-Walled Struct.*, vol. 161, 2021, 107395. doi:10.1016/j.tws.2020. 107395.

[7] S. F. Chen, "Calculation and construction of single-angle steel struts connected by one leg," *J. Archit. Civil Eng.*, vol. 25, no. 02, pp. 72-78, 2008. doi:10.3321/j.issn:1673-2049.2008.02.012.

[8] S. F. Chen, "Comments on some issues of the american specification for structural steel buildings," *Progress in Steel Building Structures.*, vol. 14, no. 06, pp. 57-62, 2012.

[9] Z. L. Li, P. Liu, and D. Y. Zhang, "Experimental research on stability of high-intensity equilateral angle Q460," in *Proc. the Seventeenth National Conference on Structural Engineering (Ⅰ)*, 2008, pp. 620-624.

[10] Z. L. Li, S. L. Shi, and D. Y. Zhang, "Local buckling of Q460 single equal-angle steel strut," *J. Shenyang Univ. Technol.*, vol. 31, no. 06, pp. 701-707, 2009, doi:CNKI:SUN:SYGY.0.2009-06-021.

[11] S. L. Shi, Z. L. Li, D. Y. Zhang, and M. H. Li, "Column curves of Q460 equal angle steel," *Power System Technology*, vol. 34, no. 09, pp. 185-189, 2010. doi:10.13335/j.1000-3673.pst.2010.09.025.

[12] Z. L. Huang, H. J. Liu, H. Y. Liu, and Z. L. Li, "Experimental study on stability behavior of equal-leg angle steel columns," *Thin-Walled Struct.*, vol. 166, 2021, 108042. doi:10.1016/j.tws.2021. 108042.

[13] W. Q. Jiang, X. Y. Chen, J. L. Liu, Z. B. Niu, L. Y. Feng, and L. Q. An, "Study on bearing capacity of transmission tower main leg with bolted joints," *Chinese Journal of Construction Machinery*, vol. 19, no. 06, pp. 471-476, 2021, doi:10.15999/j.cnki.311926. 2021.06.004

[14] DL/T 5154-2012, *Technical Code for the Design of Tower and Pole Structures of Overhead Transmission Line*, China Planning Press, Beijing, 2012.

[15] GB50017–2017, *Code for Design of Steel Structure*, China Architecture & Building Press, Beijing, China, 2017.